DuneFront

Deliverable 10.2

June 2026

DuneFront

Calibration of small-scale Living Dunes model

DuneFront – D10.2

Deliverable information

Title	Calibration of small-scale Living Dunes model
Deliverable number	10.2
WP number	10
Author(s)	Maxime Dahirel, Frederik Van Daele (UGent)
Lead beneficiary	UGent
Contributors	Malia Scoville, Jana Carus (TUBerlin)
Type	Report
Dissemination level	Public
How to cite	Dahirel, M.; Van Daele, F. (2026). DuneFront project deliverable 10.2 - Calibration of small-scale Living Dunes model
Copyright license*	© Authors and DuneFront consortium, 2024-2027. *This work is openly licensed via CC-BY.*

Versioning and contribution history

Version	Date	Authors (Institution)	Notes
Version 0.1	2026-06-02	UGent	Draft created by Beneficiary A
Version 1.0	2026-06-27	UGent	Final version approved by all Beneficiaries

Funded by the European Union. Views and opinions expressed are however those of the author(s) only and do not necessarily reflect those of the European Union. Neither the European Union nor the granting authority can be held responsible for them.

Funded by the European Union


DuneFront

DuneFront

Cover page

The goal of the DuneFront project is to develop research on Dune-Dike hybrid (DD-hybrid) Nature-based Solutions (NbS), to improve coastal protection in a context of climate change and rising sea levels. As dunes are intrinsically driven by sediment-vegetation feedbacks, efforts towards understanding and especially predicting their dynamics should ideally consider the complexity of both ecological processes and the physics of sediment transport.

The UGent team within DuneFront is making substantial strides in that direction by developing Living Dunes, a process-based model that is both physics-based and includes a detailed ecologically realistic vegetation module. This module can potentially account for multiple species, with multiple life stages, with explicit spatial spread mechanisms and context-dependency of demographic rates and key traits. All these are sources of variation that are known to be prominent in real ecological communities, important for the contribution of vegetation to dune dynamics, and yet ignored by state-of-the-art process-based models of dunes.

We here describe how Living Dunes is being parameterized using empirical data previously collected by other DuneFront partners, and present the corresponding parameter values. We then describe a proof-of-concept application of such a parameterized model, attempting to hindcast the dynamics of a small pilot dune-in-front-of-dike in Belgium, installed in 2021. By comparing model outputs and existing descriptions of the empirical sediment and vegetation dynamics at that site, we show that Living Dunes reproduces reality well, though the performance steadily degrades with time, as expected. Living Dunes is still in active development; we conclude by highlighting ongoing areas of improvement for the model, in particular around the inclusion of belowground empirical data. A well-parameterized Living Dunes model will have the potential to provide predictions about multispecies ecological dynamics and sediment dynamics simultaneously, including in response to predicted climate change. It will therefore be particularly useful to study, demonstrate or evaluate the potential co-benefits (biodiversity, coastal protection,...) of dune-dike hybrid Nature-based Solutions in a changing world.

DuneFront

Table of Content

DuneFront

List of abbreviations

Abbreviation	Explanation
NbS	Nature-based solution(s)
WP	Work package
DTM	Digital terrain model
RTK-GNSS	Real time kinematics – Global navigation satellite system
SVM	Support vector machine
SE, SD	Standard error, standard deviation

1. Introduction

1.1 Overview of DuneFront Work Package 10

The DuneFront project (https://dunefront.eu/) aims to research and mainstream dune-dike hybrids as multifunctional Nature-based Solutions (NbS) that integrate ecological processes into traditional "hard" engineered infrastructure for coastal protection and resilience.

Within DuneFront, the primary goal of Work Package (WP) 10 ("Biodiversity functioning") is to obtain a deeper knowledge of the role of biodiversity and ecological processes in shaping dune (and thus dune NbS) development and stability. More specifically, WP10 is explicitly trait-focused (in contrast with the other main biodiversity-centric DuneFront WP, **WP5**): the central idea is that variation in plant traits, at inter- and/or intraspecific levels, drives variation in the role of biodiversity in dune ecomorphodynamic feedbacks (Bonte et al., 2025; McGuirk et al., 2022; Moore et al., 2025). As standardized trait data (especially belowground trait data) are lacking for many dune plant species, the goal of WP10 is two-fold: collect new trait data that address gaps relevant to NbS functioning; use these and other trait data to better parameterize models of plant-sediment interactions and dune development.

1.2 Work Package sub-tasks, milestones and deliverables

WP10 is subdivided into three sub-WPs or tasks. **Tasks 10.1** and **10.2** were aimed at assessing the importance of plant response and effect traits, respectively. In Task 10.1, Consortium members measured "growth, expansion and fitness traits of dune-impacting species in the field, and link[ed] them to recent changes in sediment accretion-erosion" as delivered by **D6.1** (Robin et al., 2024). In **Task 10.2**, Consortium members presented the results of novel experiments aiming to link plant characteristics and sand accretion or erosion potential. Deliverable **D10.1** (Scoville et al., 2026) contains the results for both **Tasks 10.1** and **10.2**.

In **Task 10.3**, the goal is to integrate response and effect trait information, especially empirical data collected in **Tasks 10.1** and **10.2**, to parameterize a model to predict small-scale changes in the coupled vegetation-sediment dynamics. Summary statistics (milestone **M10.1**) will be made available to support various other tasks, including potentially the development of the DuneFront predictive digital twin (**WP13**). This deliverable (**D10.2**) presents the outcome of **Task 10.3**. Importantly, the parameterization presented here relates specifically to *Calamagrostis arenaria* (L.) Roth (formerly *Ammophila arenaria*), the marram grass. This *initial* focus is justified as marram grass is the dominant species, and the major dune-building species in European shifting dunes (especially in the Atlantic Biogeographic Region which is the main focus of most DuneFront research) (Bakker, 1976; Doing, 1985; Doody, 1991).

2. Methods

2.1 Overview of the model

The model to which we integrate empirical plant trait data in this deliverable is **Living Dunes**. This model, developed by the Ghent University team (https://landscape-visions.github.io/livingdunes/index.html, Van Daele & Bonte, in prep.), is an advanced (now physics-based) version of the previous DuneVeg model (Bonte et al., 2021) allowing for mechanistic, multi-species calibrations. We provide below a short and basic overview of this model; for a more thorough and detailed description of the model, its structure and capabilities, and its use, we send the reader to the above documentation.

Briefly, Living Dunes is a grid-based, process-based coastal dune model, implemented as a Python package. It is a modular framework, with different modules for each of the main aspects of the sediment-vegetation dune-building feedbacks (environmental forcing and edaphic aspects, vegetation life history and traits, sediment transport, geomorphology…). This allows for development and updates in each module without affecting the other modules or their integration.

Environmental drivers include wind, microclimate (by downscaling existing climate data), as well as soil moisture, salinity, and organic matter (Maun, 2009). The model accounts for a full series of complex aerodynamic interactions to model aeolian sand displacement (including the direct and indirect effects of both topography and the vegetation). In addition to aeolian sand transport, the model also accounts for sediment redistribution via avalanching.

In Living Dunes, ecomorphodynamic feedbacks emerge mechanistically from coupling between modules across time steps: vegetation cover, density, height and stem diameter at one time step influence sediment transport at the next step by altering the wind field (sediment transport module); sand erosion/deposition at one step influences vegetation demography (lateral and vertical growth, survival, seed production…) at the next.

Compared to existing process-based coastal dune models, Living Dunes most notably innovates by going beyond treating plants as a simplified uniform canopy layer with fixed properties, explicitly modelling dune plant life history, traits and how they may react plastically to the environmental conditions experienced. Among other things, this allows for the emergence of ecologically realistic and heterogeneous vegetation layers, with correspondingly heterogeneous impacts on sand transport, sediment-vegetation interactions, and dune dynamics.

The modular nature of the model and its Python codebase allow for full open use as well as complementary integration with other software packages (e.g. AeoLiS; van Westen et al., 2024) and digital twinning.

2.2 The need for empirical parameterization in the vegetation module

Contrary to existing process-based dune models, Living Dunes explicitly models plant demography, spatial dynamics and their impact on traits that shape ecomorphodynamics. For each included species, the vegetation module of Living Dunes thus accounts for context-dependent transitions between multiple life stages (seed, juvenile, adult). Key life-history traits such as lateral and vertical growth rates, germination, lateral spread..., as well as the resulting plant state traits (height, density...) are also modelled and potentially context-dependent. This environmental context dependence of demographic process (including, crucially, on sand burial, Maun, 2009; Bonte et al., 2021) is mirrored by the impact the resulting plant phenotypes at each grid cell influence wind speed and then sediment transport, closing the dune-building feedback loop.

In addition, the model considers the way wind may bend plant stems, influencing the effective canopy characteristics and its impact on the wind field. These impacts also depend on plant traits, namely stem and leaf structural properties.

Therefore, to parameterize Living Dunes so that it can reproduce dune dynamics in a realistic, ecologically informed way, empirically derived information about plant characteristics is ideally needed along several axes. Importantly, we primarily focus in this report on the parameters for which the current configured values are validated directly against **empirical field measurements (Table 1)**, which as of writing represent only a part of all plant-related configuration parameters. For more details on the whole configuration, including on other model parameters for which the connection between configured values and empirical data is currently less direct, see the documentation at https://landscape-visions.github.io/livingdunes/configuration/atlantic_europe/species/ammophila_arenaria/traits.html as well as Van Daele & Bonte (in prep.).

Table 1. Description of the parameters in the *Calamagrostis arenaria* configuration file that are to be substantiated by empirically collected response and effect traits from Scoville et al. (2026).

Parameter	Description
`max_height`	The maximum exposed canopy height above the sand surface. This is used as an upper bound for height growth in the plant demography module.
`height_to_stem_diameter` *a*	Parameter *a* of the relationship between canopy height and stem diameter (may be linear or power relationship)
`height_to_stem_diameter` *b*	Parameter *b* of the above relationship

`cover_to_shoot_density` *slope*	Slope of the linear relationship between (living) shoot density and fractional cover
`stem_flexibility_coefficient`	Fraction of the stem that behaves flexibly
`stem_structural_rigidity`	Fraction contributing to rigid resistance
`wind_speed_bending_threshold`	Speed at which significant bending starts
`max_height_reduction_ratio`	Maximum fraction of height lost to bending under wind conditions

2.3 Empirical data used in parameterization

Trait data used in model parameterization (**Table 2**) were collected during the summer of 2025 at four of the DuneFront sites: Sainte-Marie-la-Mer, Soulac-sur-Mer, Ostend, and Sankt Peter-Ording (**Fig. 1**). These field sessions were part of the research contributing to DuneFront deliverable D10.1 (Scoville et al., 2026).

Figure 1. Map of the sites used in this deliverable within Europe. The green and brown areas correspond to the Atlantic and Mediterranean biogeographic regions, respectively (European Environment Agency, 2002, 2016).

Table 2. List of traits used in this deliverable and their measurement descriptions. See Scoville et al. (2026) for a more complete list of all traits measured at the focal sites, as well as more details on protocols.

Trait	Unit	Details
Quadrat-level measurements:		
Plant height	cm	Depending on location: height measured from base to tallest structure, either leaf or spike (specified as `Height` in dataset), or from base to specifically tallest leaf (`Height_leaf`).
Total aboveground dry mass	g	Total aboveground biomass dried at 60°C for 48 hours
Stem density (total)	density.m^{-2}	Total number of stems living and dead (measured per 20 × 20 cm quadrat, converted in density.m^{-2})
Stem density (living)	density.m^{-2}	Same as above, but living stems only
Individual stem-level measurements:		
Stem diameter	mm	Width of stem measured 3 cm above base
E	MPa	Young's modulus or elastic modulus
I	mm^4	Second moment of area
EI	N.mm^2	Flexural rigidity, structural stiffness, stem resistance to bending
k	N.mm^{-1}	Bending stiffness
F_{max}	N	Maximum force required to bend stem

In some of the sites and for some traits, separate data collection took place in high-burial and low-burial areas, and/or in natural dunes or sites with planted marram grass (recent or older), leading in some cases to > 4 locations with data (up to 7 in data used in present deliverable, see **Table 3**). For each location (and species), aboveground measurements were done in 20 × 20 cm quadrats (between 10 and 30 per location), with additional stem mechanical traits measured on individual stems (between 24 and 89 per location) (**Table 2**).

As mentioned in the Introduction, we describe in this report results on the empirical parameterization for the marram grass *Calamagrostis arenaria* only. However, empirical data on relevant aboveground (and belowground) traits were collected for a range of additional species in that same field campaign, including other important dune-building species such as *Elytrigia juncea* (L.). The parameterization of Living Dunes for such species is an area of active development.

2.4 Statistical analyses

Analyses presented in this deliverable were done using R (R Core Team, 2025).

The dataset made available for analyses contains location-level summary statistics (means, standard deviations, sample sizes) rather than individual- or quadrat-level traits. Therefore, all analyses presented below accounted for this in one of two ways:

- When the analysis target was a single empirically measured trait, we used meta-analytic approaches to obtain overall estimates. We ran random-effect meta-analyses for both the mean and the within-location standard deviation (log-transformed) following Nakagawa et al. (2023), using the `metafor` R package (Viechtbauer, 2010). We obtained information about the between-location standard deviation from the model for the mean (τ = square root of the absolute heterogeneity).
- When the target was a relationship between two empirically measured traits, we used weighted regression approaches (with weights proportional to the inverse of the squared standard error of each location-level value).

3. Model validation case: dune-in-front-of-dike @ Ostend, Belgium

For a first validation of the Living Dunes model, we used an existing dune-in-front-of-dike pilot project, for which extensive data about sand accumulation and vegetation development were available for the first years of its installation. This pilot is located in the Oosteroever neighborhood in Ostend, Belgium (**Figure 2**), about 7 km northeast (along the coast) from the main local DuneFront demonstrator site (Living Lab Raversijde). The area (both pilot and natural surroundings) is where the Ostend empirical data mentioned in **2.3** above were collected. This pilot and its development have been extensively described in publications (Derijckere et al., 2023; Strypsteen et al., 2024); we provide below a short summary.

The beach at Oosteroever is backed by a preexisting dike. In January 2021, a 120 × 20 m^2 area in front of that dike was planted with marram grass *Calamagrostis arenaria*. That area was divided in six 20 × 20 m^2 zones, in which the density and the pattern of plantation varied: 6 plants.m^{-2} gridded, 9 plants.m^{-2} clustered, 9 plants.m^{-2} gridded, 9 plants.m^{-2} in staggered rows, 9 plants.m^{-2} random, and 15 plants.m^{-2} gridded (from South to North). This was aimed at examining both the effects of plant density and plant configuration on dune dynamics. However, a few months in, almost all planted tussocks were completely buried; recovery occurred within a few months, but in a way that made the initial differences in planting densities disappear (Strypsteen et al., 2024). The entire zone is enclosed by a steel wire fence, both to restrict access and to facilitate dune development. Approximately monthly aerial drone flights allowed the creation of high accuracy Digital Terrain Models (DTMs) for the

enclosed area and its surroundings, which have been validated against direct RTK-GNSS measurements (Strypsteen et al., 2024). They also provided orthophotographs that were used to infer vegetation cover, using an SVM-based classifier (see also Bonte et al., 2021).

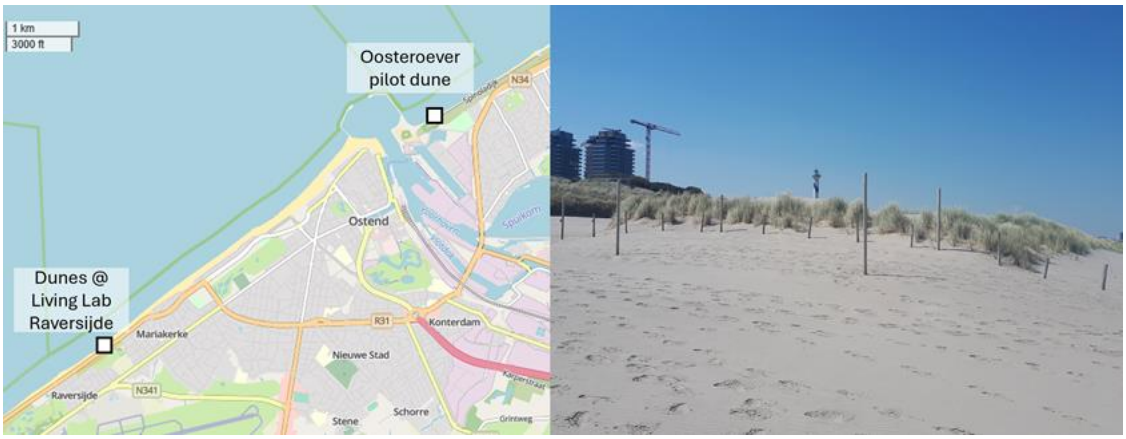

Figure 2. Left: the Oosteroever pilot dune in relation to the main DuneFront demonstrator site in the Ostend area (map from OpenStreetMap). Right: a view of the pilot dune from the east end (image by Dries Bonte).

The parameterized Living Dunes model was used to perform hindcasting simulations of this dune-in-front-of-dike system for three years starting from September 2021 (i.e. after the initial burial and recovery), at 0.2 m (spatial) and hourly (temporal) resolution. Local weather for the period was obtained from ERA5 reanalysis (wind data) and Open-Meteo (precipitation and temperature records). Pixel-wise performance of the model against existing elevation and vegetation data was evaluated through a series of indicators; we focus here on the correlation between observed and predicted value (Pearson's *r*), as well as on how well the simulation predicted the *presence* of vegetation at a pixel rather than the quantity (as measured by the F1 score).

4. Results

4.1 Empirical parameterization: Morphological traits

4.1.1 Meta-analytic summaries

The meta-analytic summaries for each trait in **Table 2** are provided below in **Table 3.** We note that for plant height, using leaf-based height measurements as a substitute in locations without direct height data does not meaningfully change the outcome (estimates are all within 1 SE of each other). Relative heterogeneities are very high for almost all traits, as

expected from ecological data (Senior et al., 2016); nonetheless, the estimated values still provide valuable guidelines for model parameterization (see next subsections).

Table 3. Meta-analysis results. Values provided are mean estimates ± SEs. For SD parameters, SEs are carried over from the original scale on which they are estimated (variance for between-location, ln(SD) for within) using the `errors` package (Ucar et al., 2018). Units are as described in **Table 2**.

Trait	Number of effect sizes	Overall mean μ	Between-location SD τ	Average within-location SD σ	Relative heterogeneity I^2 (μ; ln(σ) models)
Plant height:					
-Only direct measurements	3	88.5 ± 10	16.5 ± 9	16.5 ± 2.1	92%; 0%
-Only leaf-based measurements	5	91.3 ± 5.4	11.4 ± 4.5	15.8 ± 1.8	91.2%; 54.7%
-Composite (using leaf-based when direct not available)	7	89.4 ± 5.15	12.9 ± 4.1	16.3 ± 1.4	91.8%; 38.3%
Total aboveground dry mass	7	71.1 ± 10.3	24.2 ± 8.8	50.7 ± 4.9	80.5%; 50.7%
Stem density (total)	3	1189 ± 410	649 ± 390	681 ± 356	85.9%; 94%
Stem density (living)	3	464 ± 65.7	78 ± 84	284 ± 75.6	48.3%; 76.9%
Stem diameter	5	3.4 ± 0.1	0.3 ± 0.1	0.8 ± 0.1	86%; 66.7%
E	5	1073 ± 140	299 ± 116	705 ± 143	95.5%; 96.2%
I	5	9.4 ± 1.3	2.7 ± 1.2	9.3 ± 1.8	85.3%; 95.7%
EI	5	5815 ± 377	763 ± 329	2819 ± 205	82.8%; 69.9%
k	5	8.9 ± 0.5	1.1 ± 0.5	9.3 ± 1.8	83.6%; 78.9%
F_{max}	5	12.8 ± 0.7	1.5 ± 0.7	6.1 ± 0.4	78.8%; 64.1%

4.1.2 Parameterization choices

The retained parameter values are provided in **Table 4**. Details about substantiation are provided in the next subsections.

Table 4. Vegetation parameters for which the values chosen in the configuration are potentially informed by empirically collected field data.

Parameter	Retained value
`max_height`	1.5 m
`height_to_stem_diameter` *a*	0.0035
`height_to_stem_diameter` *b*	0.43

`cover_to_shoot_density` s (slope)	588
`stem_flexibility_coefficient`	0.4
`stem_structural_rigidity`	0.6
`wind_speed_bending_threshold`	6 $m.s^{-1}$
`max_height_reduction_ratio`	0.5

4.1.3 Maximum plant height `max_height`

Literature indicates *C. arenaria* mature stands typically reach heights up to 1.0–1.2 m (Huiskes, 1979), but taller plants are possible under specific conditions. We describe below how empirical data collected in DuneFront provide additional support for a `max_height` parameter set to 1.5 m.

To derive maximal plant height guide values from the results in **Table 3**, we have two options:

- *overall extreme:* take the overall predicted distribution of plant height values $\text{Normal}(\mu, \sqrt{\tau^2 + \sigma^2})$, and use extreme quantiles (e.g. 95 or 99% percentiles) from that distribution as targets;
- *tallest plants of an extreme population*: first pick an extreme location (e.g. the 95% quantile) from the predicted distribution of location-level means $\text{Normal}(\mu, \tau)$, and then take extreme quantiles from *that* population as targets.

We find that in either case, the 95% percentiles fall between 1.1 and 1.4m, and that values beyond 1.5m are highly unlikely even in extreme populations (**Figure 3**). This is true whether we use leaf-based height measurements or not. **This supports the choice to keep `max_height` to 1.5 m**.

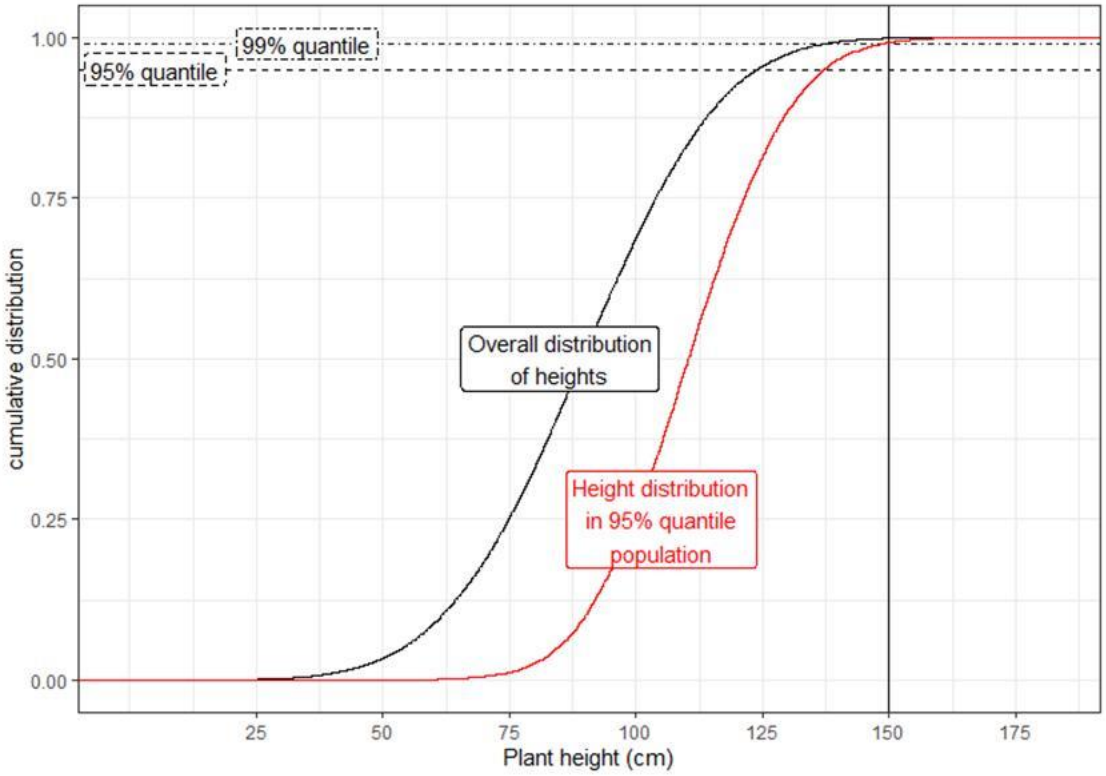

Figure 3. Cumulative distribution functions of expected individual plant heights, assuming Gaussian distribution (using "composite height" values in **Table 3**; outcomes do not meaningfully differ if using "direct height" instead). Dashed lines highlight key percentiles.

4.1.4 Allometric relationship between stem height and diameter `height_to_stem_diameter`

The allometric function `height_to_stem_diameter_function` converts exposed plant height to basal stem diameter, which in turn determines the cylinder geometry used for momentum extraction calculations.

Matching values of stem height *H* and stem diameter *D* were available for 6 locations. When both *H* and *D* are expressed in m, the relationship between the two can be modelled as the following power law: $D = 0.0035\ H^{0.43}$ ($R^2 = 0.55$, **Figure 4**).

Although height and diameter are both linear measurements and should thus scale linearly ($b = 1$) on purely geometric proportionality grounds, the fitted exponent is here <1. This means that taller plants are thinner relative to their size compared to smaller plants, which should be accounted for in modelling; this reflects the fact that grasses tend to grow primarily by elongation rather than radial extension (compared to e.g. trees). However, given the low sample size ($N = 6$ locations) and the limited height range in the data used, there is substantial

uncertainty in this exponent, with a 95% confidence interval of [0.01; 0.85]: i.e., the data as they are support nearly linear as well as nearly flat (b = 0) relationships between height and diameter. The data so far are thus also compatible with the previously encoded value of b = 0.67. The high uncertainty also explains why alternate model formulations (e.g. a simple linear model $D = a + bH$, a logarithmic model $D = a + \ln(H)$, or a square-root based model) are equally supported by the data, based on AICc values (not shown). However, the power law is the most meaningfully interpretable in biomorphological/allometric terms and is therefore the one retained in the configuration here.

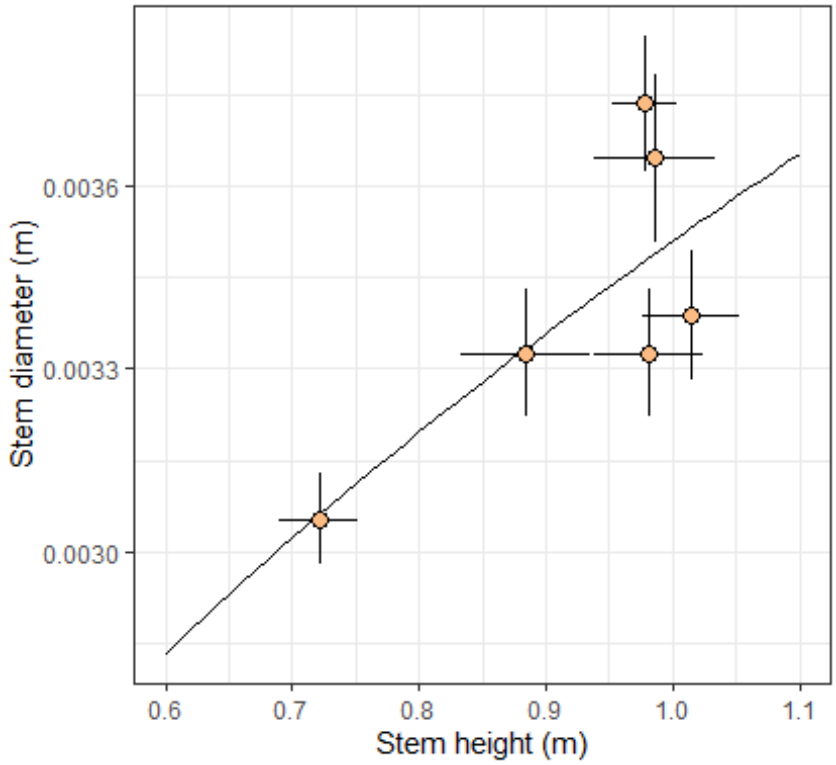

Figure 4. Relationship between stem diameter and plant height. Error bars are 1 SE.

4.1.5 Cover-to-shoot-density relationship cover `cover_to_shoot_density`

The function `cover_to_shoot_density_function` in the species configuration converts dimensionless fractional vegetation cover $c \in [0, 1]$ to tiller density ρ (in tillers.m^{-2}).

However, fractional cover was *not* directly available as of writing for the same quadrats in which density was measured, so a direct regression of density on cover was not feasible. We can sidestep this issue and recover a workable cover to shoot relationship based on empirical shoot density data by making two assumptions:

- First, that the function `cover_to_shoot_density_function` is linear: $\rho = s \cdot c + i$, with s the slope and i the intercept. Assuming here, trivially, that $i = 0$, this means $s = \rho / c$.
- Then, that the sampled quadrats were taken in dense but not monotypic canopy typical of established marram grass tussocks ($c \in [0.5, 1[$).

We can then use the mean shoot density **Table 3** to establish what values of s we should consider plausible depending on what we assume the cover c of the observed quadrats was. **Figure 5** shows that assuming the observed quadrats had an average cover of ≈ 0.8 leads to $s \approx 588$, which is used in the current parameterization. We note however that this choice is sensitive to both the chosen value of c and to variation in the mean density; as a result, plausible values span a large range (**Fig. 5**). Further measurements of both cover and shoot density may help refine parameter choices (see also potentially Lojek & Schweiger (2025) for alternative ways to obtain information on the cover-to-shoot density relationship).

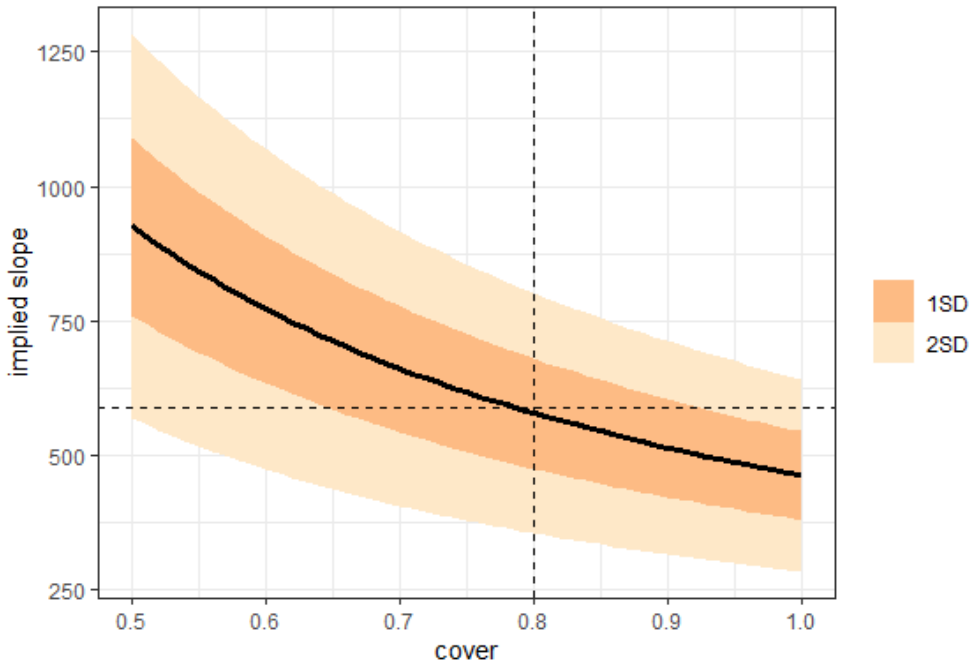

Figure 5. Expected value of the cover-to-shoot relationship slope, under a range of potential (unobserved) cover values corresponding to the observed stem densities. The dashed horizontal line corresponds to the current parameterization ($s = 588$); the color bands describe the sensitivity of the outcome to *between-location* heterogeneity in the mean shoot density **Table 3**.

4.1.6 Tiller mechanical properties

Observations made during DuneFront and related fieldwork suggest that marram grass canopies can flatten down to approximately half their standing height under strong wind, supporting a `maximum_height_reduction_ratio` value of 0.5.

Currently available mechanical traits from Scoville et al. (2026) relate to the basal culm part of the plant, whereas it is the mechanical properties of the upper leaf part of the tiller, and the relations between the two, that are most relevant for `stem_flexibility_coefficient`, `stem_structural_rigidity`, `wind_speed_bending_threshold`, and other mechanical parameters. Therefore, while these data summaries are provided here as empirical information (**Table 3**), and to support potential alternative modelling approaches, they are not used directly in the current Living Dunes configuration. Instead, the configuration primarily relies on data from published studies, that include/account for the mechanical properties of tiller leaves in addition to the basal part of the plant (Kosmalla et al., 2025; Laporte-Fauret et al., 2024); see https://landscape-visions.github.io/livingdunes/index.html and Van Daele & Bonte (2026).

4.2 Demographic response parameters - Literature-based parameterization

In addition to the morphological parameters substantiated from empirical data (**4.1** above), the *C. arenaria* configuration also includes demographic response parameters that are directly sourced from existing empirical literature, including by members of the DuneFront consortium. We provide below in **Table 4** a summary of these parameters, along with the relevant sources.

Table 4. Summary of the key demographic response parameters in the *C. arenaria* configuration file that are primarily derived from **empirical field data** in published papers with DuneFront members as (co-)authors. For more details and other parameters, see https://landscape-visions.github.io/livingdunes/index.html and Van Daele & Bonte (in prep.).

Parameter or function	Value	Description
Burial growth optimum	31 $cm.yr^{-1}$	The height growth response to burial follows a Gaussian curve, centered on this burial intensity value. See Bonte et al. (2021) and Scoville et al. (2026).
Mortality = f(Burial)	$1/(1+\exp(-k(x-t))$, with k = 0.2 and t = 65cm	Supported by Bonte et al. (2021) describing an upper tolerance to burial in the 78-96 $cm.yr^{-1}$ range. This sigmoid curve places the LD_{50}

		(burial leading to 50% mortality = t) below this tolerance limit, and places an LD_{95} at $\approx t + 3/k = 80$, within this range.
Lévy exponent	1.98	Describes the inter-tiller distance distribution of clonally expanding plants, assuming a truncated power law. Taken directly from Reijers et al. (2019).
Germination depth optimum	0.5 – 3 cm	Germination success rapidly declines if seeds are buried deeper; taken directly from Lammers, Schmidt, et al. (2024).

4.3 Model test case: summary

Importantly, the main goal of this deliverable is not to present a thorough evaluation of the hindcast performance (Van Daele & Bonte, in prep.), but to describe its parameterization. Therefore, we only provide here a rapid overview, highlighting the potential of Living Dunes.

Selected snapshots of the simulation at various dates are presented **Figure 6**.

The simulation recovers broad patterns in the development of the Oosteroever pilot that have been described in Strypsteen et al. (2024).

For instance, the model suggests that the highest points of the dunes were ≈ 1.5 m higher in early 2024 compared to late 2021 (**Figure 7**), a close match to observed patterns.

While it does underestimates it (≈ 15 m^3/m of shoreline between late 2021 and early 2024, vs. closer to 20 over the same period in Strypsteen et al. (2024)), the model broadly recover the observed patterns in total dune volume increase (note that the simulated period, and thus the comparison, does not include the early months post-plantation, during which a substantial part of the total volume change since the creation of the pilot occurred). Dune volume changes per month reached 1 m^3/m in winter months, and were much lower but never negative in summer months (**Figure 8**): this again closely matches empirical patterns described in Strypsteen et al. (2024). However, the model notably fails to recover the one period of outright erosion in the empirical dataset, around the time of storm Corrie in early 2022.

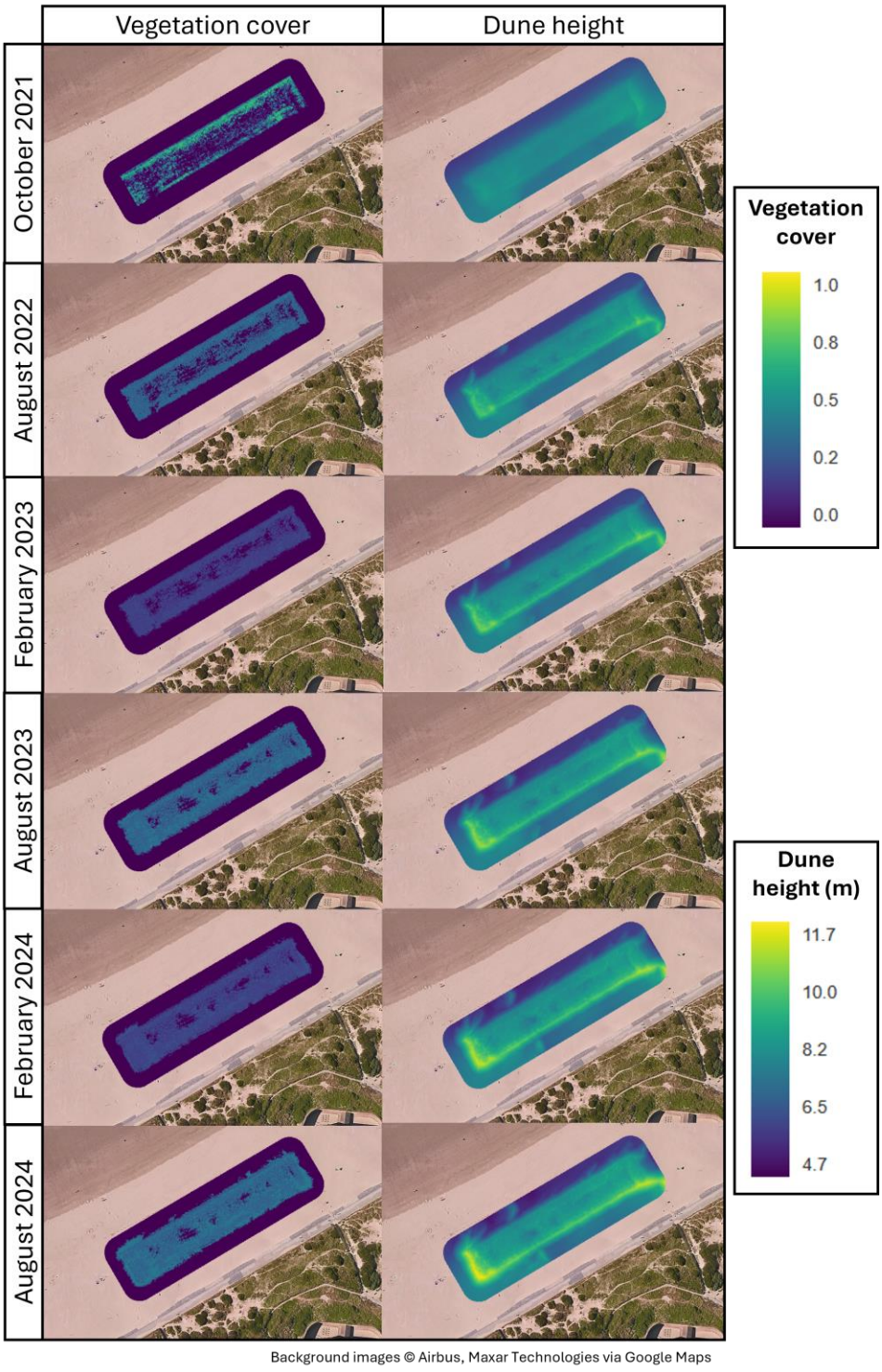

Figure 6. Selected temporal snapshots of vegetation cover and height (DTM) in the simulated dune.

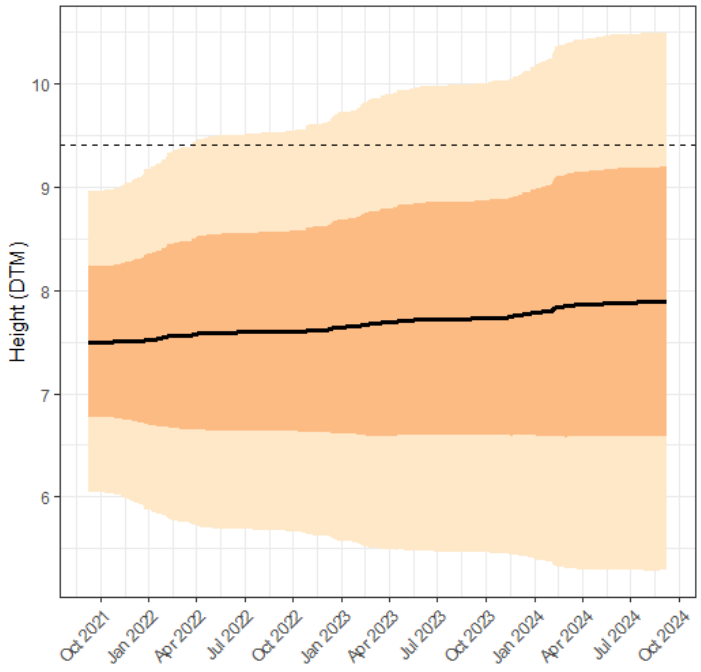

Figure 7. Temporal variation in average (± 1 and 2 SDs) pixel-level DTM height, as simulated by Living Dunes.

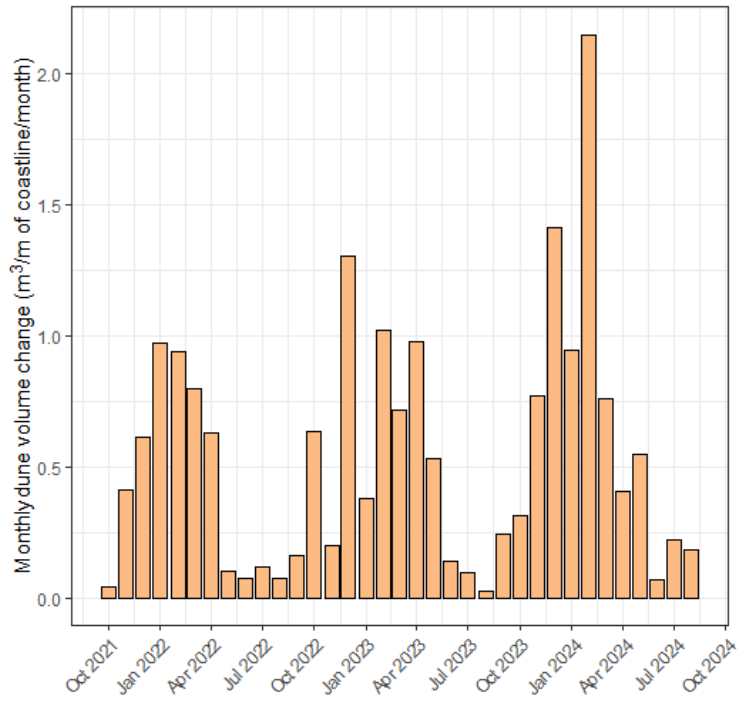

Figure 8. Monthly changes in total dune volume as simulated by Living Dunes.

The model recovers matching seasonal dynamics in exposed vegetation cover (growth in spring/summer, reduction caused by burial in winter, **Figure 9**), confirming that they can be appear as emergent without being modelled explicitly, solely from the context-dependency of plant demography and plant-sediment feedback.

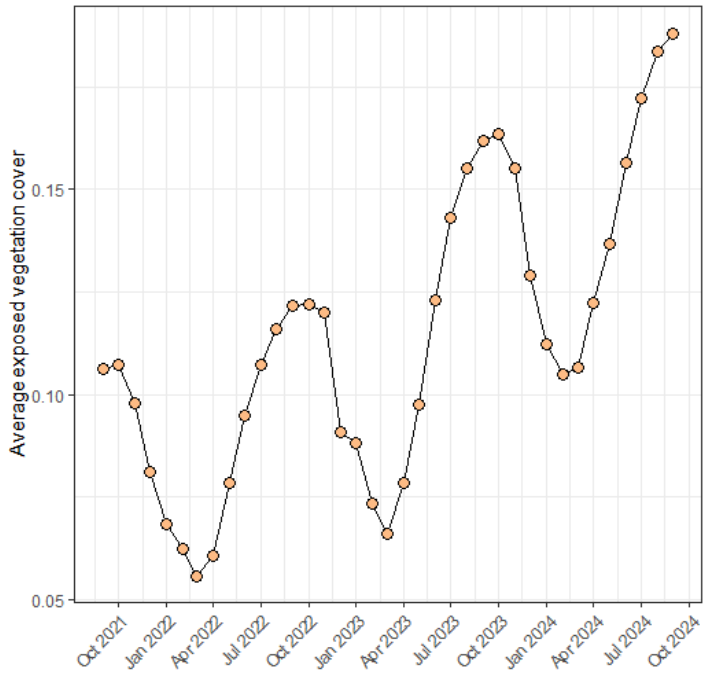

Figure 9. Temporal variation of average vegetation cover across the simulated dune.

The ability of the model to match empirical observations includes more idiosyncratic, qualitative patterns. In particular, Living Dunes reproduces the tendency for higher vegetation growth and accretion closer to the fences compared to the rest of the pilot (**Figure 6**). It also recovers the erosion immediately in front of the dune, that parallels accretion in the dune itself (**Figure 6**).

The model pixel-wise performance was initially good in the first few months, but steadily degraded with time since the initialisation of the simulation (**Figure 10**). This is a common issue for ecological prediction in general (Petchey et al., 2015). Part of the accumulated divergence between the model and empirical data might be due to non-modelled interventions: in particular, the excess sand between the fenced dune and the sea wall was occasionally taken away by cranes and bulldozers, and pushed towards the intertidal beach (Strypsteen et al., 2024). Nonetheless, ongoing refinements in parameterization may help push the forecast horizon farther (see **Perspectives** below). Performance as measured by the pixel-wise correlation coefficient degraded much faster for vegetation cover than for the DTM (**Figure 10**). However, when looking at whether the model correctly predicts *presence* of vegetation at a pixel rather than the coverage, the model's performance (as measured by

the F1 score) is much more consistent through time (**Figure 11**). The discrepancy between the two indicators for vegetation may result from the fact that most of the dune ends up covered in vegetation (**Figure 6**), making correct prediction of presence/absence much easier on average than prediction of actual cover.

However and more importantly, all this pertains to the model **pixel-wise** performance (with a 0.2 m resolution). Plant demography (including their spatial expansion strategies) being modelled explicitly introduces major stochasticity elements that may accumulate through time and lead to (relatively) bad pixel-wise measures of performance (the odds of new tillers sprouting exactly where they did in reality being infinitesimal). This, *even though the patterns at broader spatial scales may be matched much more closely* (see for instance how the model correctly recovered differences between close and away from the fences). Future multi-scale evaluation procedures may provide a much better-balanced picture of Living Dunes' performance.

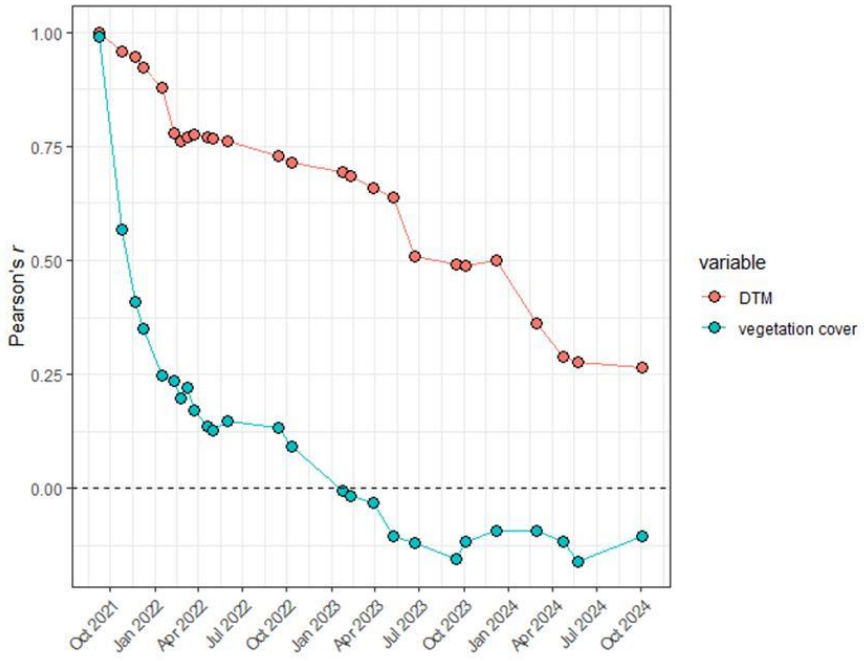

Figure 10. Temporal variation in simulation performance, as measured by the Pearson correlation coefficient. For time points where they are available, the model output is compared to the observed empirical data on sediment accumulation and vegetation cover.

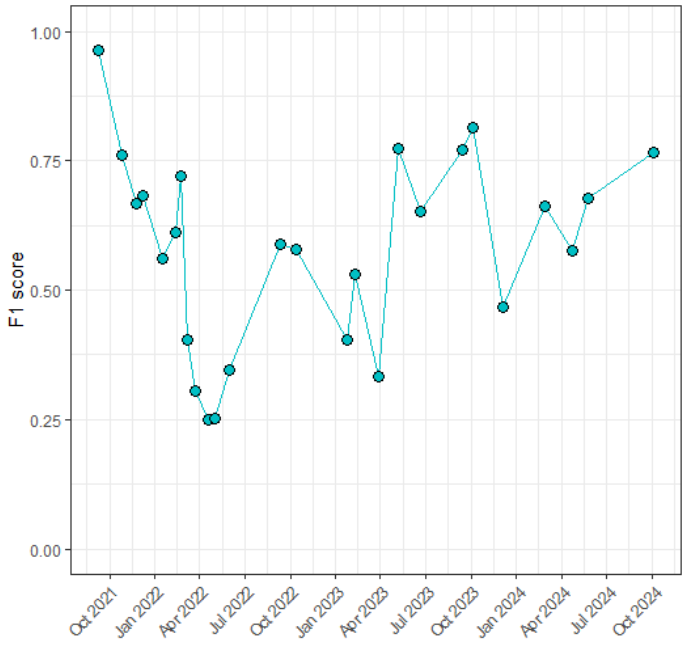

Figure 11. Temporal variation in simulation performance for vegetation cover, as measured by the F1 score. For time points where they are available, the model output is compared to the observed empirical data on vegetation cover.

5. Perspectives

Living Dunes is in active development, and trait data collection/analysis within DuneFront is continuing. The present deliverable reflects model state and empirical data availability as of writing and may change at later dates. Within DuneFront, a well-parameterized Living Dunes model has the potential to contribute to other work packages, in particular (but not only) by providing or validating Technical Key Target Indicators for the development of blueprints and Decision Support Systems (Hassanpour et al., 2026). Some potential avenues for improvement *in relation to empirical parameterization* include the following:

- So far, model parameterization has relied only on aboveground trait data. Roots may play an important yet poorly understood role in dune dynamics, especially regarding their stability against erosion (De Battisti & Griffin, 2020; Figlus et al., 2022; Kosmalla et al., 2026). Data collection in Scoville et al. (2026) included several belowground traits. Combined with physical experiments accounting for belowground development in other DuneFront work packages (Lojek & Schweiger, 2026), these may provide a basis for a better parameterization of belowground traits in Living Dunes (going

beyond the current status quo that e.g. assumes a symmetry between root and shoot, with similar maximal heights/depths and a biomass ratio of 0.5).

- The current parameterization assumes the same set of "average" parameters applies independently of context. The role of intraspecific variation for ecosystem functioning is increasingly recognized, both within and between populations (Siefert et al., 2015; Westerband et al., 2021). The high meta-analytic heterogeneity seen in **Table 3** supports the idea this should be something to account for; however, one must keep in mind that the number of effect sizes was low. Extensive field data collection across a wider range of European sites is ongoing, and the Living Dunes model can already easily accommodate biogeographical-level variation in relevant traits or functional relationships (via using different configuration files to initiate simulations depending on biogeographical region). Preliminary analyses suggest that the effect of within-location variation in traits (due to dune age, planted vs natural, high vs low dynamics… ; Scoville et al., 2026) is already accounted for, at least partly, by the context-dependency of plant demography (Van Daele & Bonte, in prep.), though this could also be improved. Sensitivity and robustness analyses will be used to determine how different sources of heterogeneity may affect outcomes. Ultimately though, some part of this heterogeneity will remain irreducible, especially at the pixel level; the ability to embrace and highlight that uncertainty, rather than ignore it, is a feature, not a bug, of Living Dunes.

- Current tests only account for the marram grass *Calamagrostis arenaria*. While it is the dominant dune-building grass on most of the European coastline, it is not the only one (Bakker, 1976; Doing, 1985; Doody, 1991). *C. arenaria* and *Elytrigia juncea* create dunes with different sizes and shapes, and their interactions when both are present may have complex impacts on dune dynamics (Lammers, Reijers, et al., 2024). In more northern dunes, *C. arenaria* may be replaced in part or all by *Leymus arenarius*, again potentially influencing dune dynamics. Finally, while they are not as abundant and likely do not play as much as a role quantitatively speaking, non-grass species such as *Cakile maritima* may also contribute to sand trapping (Davy et al., 2006; Scoville et al., 2026). The Living Dunes model allows the simulation of multispecies communities, providing unique opportunities to investigate the impact of vegetation on dune dynamics in an ecologically realistic fashion. Here again, relevant data either have been (Scoville et al., 2026) or are being actively collected by DuneFront consortium teams, making this an achievable goal in the near future.

6. References

Bakker, J. P. (1976). Phytogeographical aspects of the vegetation of the outer dunes in the Atlantic province of Europe. *Journal of Biogeography*, *3*(2), 85–104. https://doi.org/10.2307/3038138

Bonte, D., Koedooder, C., Taelman, C., & DuneFront Consortium. (2025). *DuneFront Policy Brief: Rewilded coasts, mainstreaming biodiversity in Nature-based Solutions for coastal management*. https://vliz.be/en/imis?module=ref&refid=437118

Bonte, D., Batsleer, F., Provoost, S., Reijers, V., Vandegehuchte, M. L., Van De Walle, R., Dan, S., Matheve, H., Rauwoens, P., Strypsteen, G., Suzuki, T., Verwaest, T., & Hillaert, J. (2021). Biomorphogenic feedbacks and the spatial organization of a dominant grass steer dune development. *Frontiers in Ecology and Evolution*, *9,* 761336. https://doi.org/10.3389/fevo.2021.761336

Dahirel, M., & Bonte, D. (2025). *DuneFront deliverable D4.2 - Biological boundary conditions*. Zenodo. https://doi.org/10.5281/zenodo.15044553

Davy, A. J., Scott, R., & Cordazzo, C. V. (2006). Biological flora of the British Isles: *Cakile maritima* Scop. *Journal of Ecology*, *94*(3), 695–711. https://doi.org/10.1111/j.1365-2745.2006.01131.x

De Battisti, D., & Griffin, J. N. (2020). Below-ground biomass of plants, with a key contribution of buried shoots, increases foredune resistance to wave swash. *Annals of Botany*, mcz125. https://doi.org/10.1093/aob/mcz125

Derijckere, J., Strypsteen, G., & Rauwoens, P. (2023). Early-stage development of an artificial dune with varying plant density and distribution. *Geomorphology*, *437*, 108806. https://doi.org/10.1016/j.geomorph.2023.108806

Doing, H. (1985). Coastal fore-dune zonation and succession in various parts of the world. *Vegetatio*, *61*(1), 65–75. https://doi.org/10.1007/BF00039811

Doody, J. P. (Ed.). (1991). *Sand dune inventory of Europe*. Joint Nature Conservation Committee.

European Environment Agency. (2002). *Europe's biodiversity - biogeographical regions and seas*. https://www.eea.europa.eu/en/analysis/publications/report_2002_0524_154909

European Environment Agency. (2016). *Biogeographical Regions of Europe, version 2016* [Dataset]. https://www.eea.europa.eu/en/datahub/datahubitem-view/11db8d14-f167-4cd5-9205-95638dfd9618

Figlus, J., Sigren, J. M., Feagin, R. A., & Armitage, A. R. (2022). The unique ability of fine roots to reduce vegetated coastal dune erosion during wave collision. *Frontiers in Built Environment*, *8*, 904837. https://doi.org/10.3389/fbuil.2022.904837

Hassanpour, N., Stratigaki, V., El Rahi, J., Bonte, D., Sterckx, T., & Huygens, M. (2026). *DuneFront deliverable D14.1 - Developing the Blueprint Guideline for DD-hybrid Nature-based Solutions*.

Huiskes, A. H. L. (1979). *Ammophila arenaria* (L.) Link (*Psamma arenaria* (L.) Roem. et Schult.; *Calamagrostis arenaria* (L.) Roth). *Journal of Ecology*, *67*(1), 363–382. https://doi.org/10.2307/2259356

Kosmalla, V., Lojek, O., Ahrenbeck, L., Mehrtens, B., Schweiger, C., Schürenkamp, D., & Goseberg, N. (2026). Vegetation effects on dune erosion under wave collision: Influence of planting density, biomass distribution and arrangement in scaled experiments. *Coastal Engineering*, *204*, 104899. https://doi.org/10.1016/j.coastaleng.2025.104899

Kosmalla, V., Lojek, O., Carus, J., Keimer, K., Ahrenbeck, L., Mehrtens, B., Schürenkamp, D., Schröder, B., & Goseberg, N. (2025). Biomechanical parameters of marram grass (*Calamagrostis arenaria*) for advanced modeling of dune vegetation. *Earth Surface Dynamics*, *13*(5), 791–825. https://doi.org/10.5194/esurf-13-791-2025

Lammers, C., Reijers, V. C., & van der Heide, T. (2024). Scale-dependent interactions in coastal biogeomorphic landscapes: Pioneer both inhibits and facilitates primary foredune builder across spatial scales. *Geomorphology*, *467*, 109486. https://doi.org/10.1016/j.geomorph.2024.109486

Lammers, C., Schmidt, A., van der Heide, T., & Reijers, V. C. (2024). Habitat modification by marram grass negatively affects recruitment of conspecifics. *Oecologia*, *204*(3), 705–715. https://doi.org/10.1007/s00442-024-05525-y

Laporte-Fauret, Q., Wengrove, M., Ruggiero, P., Hacker, S. D., Cohn, N., Zarnetske, P. L., & Piercy, C. D. (2024). A new approach to account for species-specific sand capture by plants in an aeolian sediment transport and coastal dune building model. *Journal of Geophysical Research: Earth Surface*, *129*(12), e2024JF007867. https://doi.org/10.1029/2024JF007867

Lojek, O., & Schweiger, C. (2025). *DuneFront deliverable D6.3 - Environmental influences*. https://www.vliz.be/nl/imis?module=ref&refid=418886

Lojek, O., & Schweiger, C. (2026). *DuneFront deliverable D12.2 - Physical modelling of the German Demonstrator*.

Maun, M. A. (2009). *The biology of coastal sand dunes*. Oxford University Press.

McGuirk, M. T., Kennedy, D. M., & Konlechner, T. (2022). The role of vegetation in incipient dune and foredune development and morphology: a review. *Journal of Coastal Research*, *38*(2), 414–428. https://doi.org/10.2112/JCOASTRES-D-21-00021.1

Moore, L. J., Hacker, S. D., Breithaupt, J., De Vries, S., Miller, T., Ruggiero, P., & Zinnert, J. C. (2025). Ecomorphodynamics of coastal foredune evolution. *Nature Reviews Earth & Environment*, *6*(6), 417–432. https://doi.org/10.1038/s43017-025-00672-z

Nakagawa, S., Yang, Y., Macartney, E. L., Spake, R., & Lagisz, M. (2023). Quantitative evidence synthesis: a practical guide on meta-analysis, meta-regression, and publication bias tests for environmental sciences. *Environmental Evidence*, *12*(1), 8. https://doi.org/10.1186/s13750-023-00301-6

Pérez-Harguindeguy, N., Díaz, S., Garnier, E., Lavorel, S., Poorter, H., Jaureguiberry, P., Bret-Harte, M. S., Cornwell, W. K., Craine, J. M., Gurvich, D. E., Urcelay, C., Veneklaas, E. J., Reich, P. B., Poorter, L., Wright, I. J., Ray, P., Enrico, L., Pausas, J. G., de Vos, A. C., … Cornelissen, J. H. C. (2013). New handbook for standardised measurement of plant functional traits worldwide. *Australian Journal of Botany*, *61*(3), 167–234. https://doi.org/10.1071/BT12225

Petchey, O. L., Pontarp, M., Massie, T. M., Kéfi, S., Ozgul, A., Weilenmann, M., Palamara, G. M., Altermatt, F., Matthews, B., Levine, J. M., Childs, D. Z., McGill, B. J., Schaepman, M. E., Schmid, B., Spaak, P., Beckerman, A. P., Pennekamp, F., & Pearse, I. S. (2015). The ecological forecast horizon, and examples of its uses and determinants. *Ecology Letters*, *18*(7), 597–611. https://doi.org/10.1111/ele.12443

R Core Team. (2025). *R: a language and environment for statistical computing* (Version 4.5.1) [Computer software]. R Foundation for Statistical Computing. https://www.R-project.org/

Reijers, V. C., Siteur, K., Hoeks, S., van Belzen, J., Borst, A. C. W., Heusinkveld, J. H. T., Govers, L. L., Bouma, T. J., Lamers, L. P. M., van de Koppel, J., & van der Heide, T. (2019). A Lévy expansion strategy optimizes early dune building by beach grasses. *Nature Communications*, *10*(1), Article 1. https://doi.org/10.1038/s41467-019-10699-8

Robin, N., Ruz, M.-H., Castelle, B., & Blaise, E. (2024). *DuneFront deliverable D6.1 - Morphodynamics patterns*. https://www.vliz.be/en/imis?module=ref&refid=409899

Scoville, M., Carus, J., Taelman, C., & Reijers, V. (2026). *DuneFront deliverable 10.1 - Assessing plant traits*.

Senior, A. M., Grueber, C. E., Kamiya, T., Lagisz, M., O'Dwyer, K., Santos, E. S. A., & Nakagawa, S. (2016). Heterogeneity in ecological and evolutionary meta-analyses: its magnitude and implications. *Ecology*, *97*(12), 3293–3299. https://doi.org/10.1002/ecy.1591

Siefert, A., Violle, C., Chalmandrier, L., Albert, C. H., Taudiere, A., Fajardo, A., Aarssen, L. W., Baraloto, C., Carlucci, M. B., Cianciaruso, M. V., de L. Dantas, V., de Bello, F., Duarte, L. D. S., Fonseca, C. R., Freschet, G. T., Gaucherand, S., Gross, N., Hikosaka, K., Jackson, B., … Wardle, D. A. (2015). A global meta-analysis of the relative extent of intraspecific trait variation in plant communities. *Ecology Letters*, *18*(12), 1406–1419. https://doi.org/10.1111/ele.12508

Strypsteen, G., Bonte, D., Taelman, C., Derijckere, J., & Rauwoens, P. (2024). Three years of morphological dune development after planting marram grass on a beach. *Earth Surface Processes and Landforms*, *49*(10), 2980–2997. https://doi.org/10.1002/esp.5870

Ucar, I., Pebesma, E., & Azcorra, A. (2018). Measurement errors in R. *The R Journal*, *10*(2), 549–557. https://doi.org/10.32614/RJ-2018-075

Van Daele, F., & Bonte, D. (in prep.). *Living Dunes: A process-based model coupling aeolian sediment transport and plant demography for coastal resilience* [Unpublished manuscript].

van Westen, B., de Vries, S., Cohn, N., van IJzendoorn, C., Strypsteen, G., & Hallin, C. (2024). AeoLiS: Numerical modelling of coastal dunes and aeolian landform development for real-world applications. *Environmental Modelling & Software*, *179*, 106093. https://doi.org/10.1016/j.envsoft.2024.106093

Viechtbauer, W. (2010). Conducting meta-analyses in R with the `metafor` package. *Journal of Statistical Software*, *36*, 1–48. https://doi.org/10.18637/jss.v036.i03

Westerband, A. C., Funk, J. L., & Barton, K. E. (2021). Intraspecific trait variation in plants: a renewed focus on its role in ecological processes. *Annals of Botany*, *127*(4), 397–410. https://doi.org/10.1093/aob/mcab011


DuneFront